Electronic Supplementary Material (ESI) for Journal of Analytical Atomic Spectrometry.
This journal is © The Royal Society of Chemistry 2019

# Electronic Supplementary Information

# Combination of $^{47}$Ti and $^{48}$Ti for the determination of highly polydisperse $TiO_2$ particle size distributions by spICP-MS

Guillaume Bucher and François Auger

Service Commun des Laboratoires, 3 Avenue Dr Albert Schweitzer, 33600 Pessac, France

## Contents

- **Preparation of sample B1** - Enrichment procedure for large $TiO_2$ particles
- **Additional information regarding sample preparation for spICP-MS analysis**
- **Table S1:** Typical spICP-MS operational parameters
- **Validation of the 60 nm and 40 nm AuNPs suspensions used for TE determination and drift control**
- **Additional information regarding potential $^{48}$Ca isobaric interference on $^{48}$Ti**
    - **Table S2:** Ca and Ti contents in samples A1, A2 and A3 supernatants which were subjected to spICP-MS analysis
- **Table S3:** Example of a typical spICP-MS analytical sequence
- **Additional data regarding sample preparation and spICP-MS analysis reliability and repeatability**
    - **Table S4:** Figures of repeatability obtained for in-house E171 additive premix used as spICP-MS control sample
    - **Table S5:** Figures of repeatability and reliability (vs. SEM measurement) obtained by spICP-MS for a typical chewing gum tablet with white coating
    - **Table S6:** Figures of repeatability and reliability vs. SEM measurement obtained by spICP-MS for a typical chocolate candy with peanut core and colored coating
- **Determination of $SiO_2$ content and particle concentrations in silica suspensions by ICP-OES**
    - **Table S7:** $SiO_2$ and particle concentrations in silica suspensions
- **Sample B1 analysis with 10 millisecond dwell time (including Figure S1)**
- **Table S8:** Physico-chemical properties of Ti, $TiO_2$, Si and $SiO_2$
- **Figure S2:** Illustration of spICP-MS signal saturation

**Preparation of sample B1**

Enrichment procedure for large $TiO_2$ particles (≈ 200-500 nm) contained in coconut syrup (A1) derived from centrifugation equations given in Gimbert *et al.* (2005).

Sample A1 was first diluted 10 times with ultrapure water to reduce its viscosity and match roughly that of ultrapure water. The diluted solution (A1D) was then sonicated for 10 min (ultrasonic bath with 45 kHz frequency and 180 W maximum absorbed power) and centrifuged as follows:

**Step 1:** Centrifugation of (A1D) with ≈ 1.2 µm minimal cutoff (*i.e.* centrifugal force gradient in the sample (from tube bottom to liquid surface) ranging from 200 to 400 g for 2 min at 20°C) → recuperation of the supernatant (A1S1) containing $TiO_2$ particles mainly smaller than 0.6 - 1.2 µm

**Step 2:** Centrifugation of (A1S1) with ≈ 0.42 µm minimal cutoff (*i.e.* centrifugal force gradient in the sample (from tube bottom to liquid surface) ranging from 1400 to 2800 g for 2 min at 20°C) → discard supernatant containing $TiO_2$ particles smaller than 0.2 - 0.4 µm and re-suspension of the pellet containing $TiO_2$ particles mainly between 0.2 and 1.2 µm by addition of ultrapure water and vigorous mixing (vortex) resulting in suspension (A1S2).

**Step 3:** repetition of Step 2 with suspension (A1S2) to retrieve suspension (A1S3)

**Step 4:** repetition of Step 2 with suspension (A1S3) to retrieve final suspension (A1S4) = sample B1

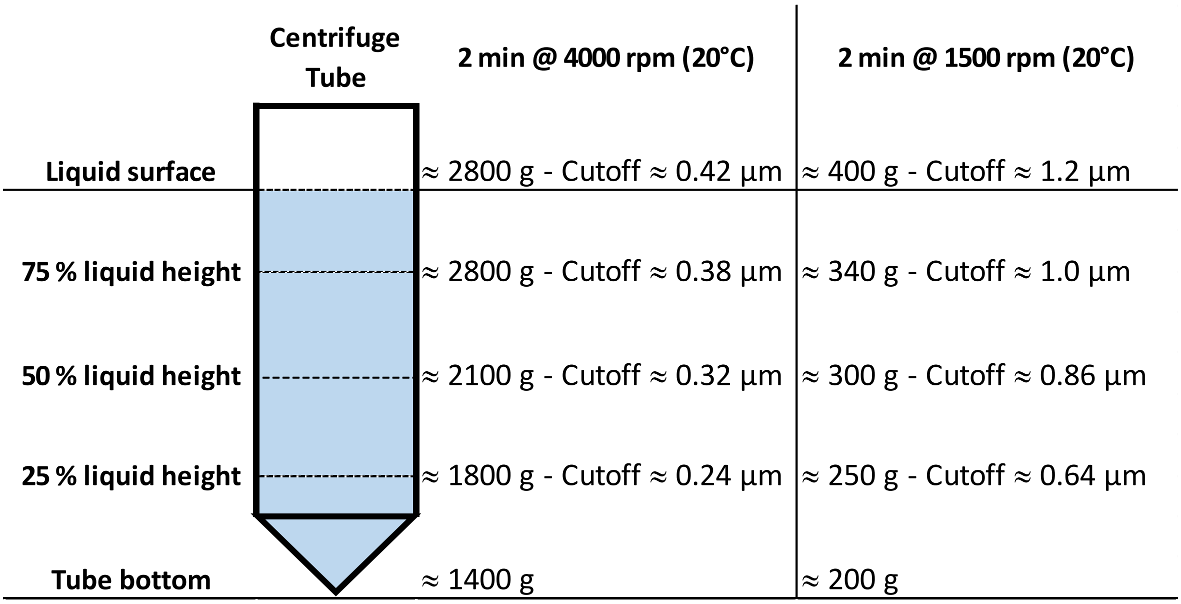

| | Centrifuge Tube | 2 min @ 4000 rpm (20°C) | 2 min @ 1500 rpm (20°C) |
|---|---|---|---|
| Liquid surface | | ≈ 2800 g - Cutoff ≈ 0.42 µm | ≈ 400 g - Cutoff ≈ 1.2 µm |
| 75 % liquid height | | ≈ 2800 g - Cutoff ≈ 0.38 µm | ≈ 340 g - Cutoff ≈ 1.0 µm |
| 50 % liquid height | | ≈ 2100 g - Cutoff ≈ 0.32 µm | ≈ 300 g - Cutoff ≈ 0.86 µm |
| 25 % liquid height | | ≈ 1800 g - Cutoff ≈ 0.24 µm | ≈ 250 g - Cutoff ≈ 0.64 µm |
| Tube bottom | | ≈ 1400 g | ≈ 200 g |

## Additional information regarding sample preparation for spICP-MS analysis.

As sample A1 was already in a liquid form (syrup), it was simply diluted 10 times prior to sonication and centrifugation as described in the manuscript (section 2.2). Samples A2 and A3 both contained E171 additive in their coating, therefore the outer layer of these samples was simply separated from the almond or jellified core by swirling in ultrapure water for about 5 minutes prior to sonication and centrifugation of the resulting suspension as described in the manuscript (section 2.2).

**Table S1: Typical spICP-MS operational parameters**

| Parameter | Value |
|---|---:|
| **Plasma Gas Flow (L min$^{-1}$)** | 18.0 |
| **Auxiliary Gas Flow (L min$^{-1}$)** | 1.20 |
| **Nebulizer Gas Flow[a] (L min$^{-1}$)** | 1.00 |
| **RF Power (W)** | 1500 |
| **Sampling Depth (mm)** | 0.0[b] |
| **Sample Uptake[c] (mL min$^{-1}$)** | 0.175 |
| **RPq (V)** | 0.45 |
| **Deflector Voltage (V)** | -11 |
| **Quadrupole Rod Offset (V)** | 0.0 |
| **Torch Injector Inner Diameter (mm)** | 1.8 |
| **Nebulizer** | Micromist 0.4 mL min$^{-1}$ |
| **Spray Chamber** | Cyclonic (glass) at room temperature |
| **Sampler, skimmer, hyperskimmer cone** | nickel |
| **Uptake tubing** | PVC 0.38 mm internal diameter |
| **Drain tubing** | Santoprene 1.30 mm internal diameter |

[a] Nebulizer Gas Flow optimized daily

[b] Position relative to the initial torch sampling depth set with Perkin Elmer's torch alignment tool

[c] Sample Uptake measured gravimetrically daily

## Validation of the 60 nm and 40 nm AuNPs suspensions used for TE determination and drift control

Since well characterized NIST AuNPs reference materials (RM) were not available at the time of this study, 60 nm and 40 nm AuNPs suspensions from BBI Solutions (Crumlin, UK) were used for TE determination and independent drift control (sizing and counting), respectively. Therefore, in order to make sure that BBI's 60 nm AuNPs suspension was reliable as a TE standard, we successfully took part in RIKILT's proficiency testing (Wageningen University & Research, The Netherlands) for size (z-score = 0.15) and particle concentration (z-score = 0.03) determination by spICP-MS in 2018. Additionally, we have also successfully determined the size of several other AuNPs suspensions including 20, 40, 80 and 100 nm AuNPs from BBI Solutions (Crumlin, UK) and 30 nm AuNPs from NIST (RM 8012).

## Additional information regarding potential $^{48}Ca$ isobaric interference on $^{48}Ti$

Samples A1, A2 and A3 supernatants (*i.e.* fractions < 1.2 µm subjected to spICP-MS analysis) were analyzed by conventional ICP-MS after acidic digestion for total Ti and Ca determination in order to determine the extent of $^{48}Ca$ isobaric interference on $^{48}Ti$. The results presented in Table S2 showed a $^{48}Ca/^{48}Ti$ ratio below 0.1% for samples A1 and A2 and around 0.5% for sample A3 which contained about 10-times less $TiO_2$ compared to samples A1 and A2. These results demonstrated that $^{48}Ca$ isobaric interference on $^{48}Ti$ could be neglected for these samples even without using the ICP-MS collision cell. Additionally, the presence of Ca (and therefore 0,187% $^{48}Ca$) or S (and therefore potentially $^{32}S^{16}O$) would essentially result in elevated ionic ("dissolved") background. The "dissolved" $^{48}Ti$ concentration (included in the result summary from the Syngistix software) was carefully monitored and was systematically much lower than 0.05 µg $L^{-1}$ when the appropriate dilution factor was achieved (*i.e.* $TiO_2$ concentration about 1.5 to 10 µg $L^{-1}$).

**Table S2: Ca and Ti contents in samples A1, A2 and A3 supernatants which were subjected to spICP-MS analysis**

| Sample | Total Ca[a] content (µg/g) | $^{48}Ca$ content[b] (µg/g) | Total Ti[c] [$TiO_2$][d] content (µg/g) | $^{48}Ti$ content[e] (µg/g) | $^{48}Ca/^{48}Ti$ ratio (%) |
|---|---|---|---|---|---|
| **A1** | 113 | 0.214 | 448 [747] | 330 | 0.06% |
| **A2** | 41.7 | 0.079 | 420 [700] | 309 | 0.03% |
| **A3** | 77.0 | 0.146 | 39.3 [65.5] | 29.0 | 0.51% |

[a] Total Ca content determined by ICP-MS using $^{44}Ca$ isotope and He collision gas

[b] Considering $^{48}Ca$ isotopic abundance of 0.187%

[d] Total Ti content determined by ICP-MS using $^{47}Ti$ isotope and He collision gas

[d] Considering $Ti/TiO_2$ mass fraction of 59.9%

[e] Considering $^{48}Ti$ isotopic abundance of 73.72%

**Table S3: Example of a typical spICP-MS analytical sequence**

| **Sample** | **Analyte** | **Run time (s)** | **Verifications** |
|---|---|---|---|
| ST0 Au (Blank) | $^{197}$Au | 60 | 197Au ionic calibration<br>Linearity<br>**R² ≥ 0,999** |
| ST1 Au (1 ppb) | $^{197}$Au | 60 | |
| ST2 Au (5 ppb) | $^{197}$Au | 60 | |
| ST3 Au (10 ppb) | $^{197}$Au | 60 | |
| Blank AuNP | $^{197}$Au | 60 | |
| 60 nm AuNP STANDARD | $^{197}$Au | 60 | |
| 40 nm AuNP CONTROL #1 | $^{197}$Au | 60 | Size recovery : **95 – 105 %** |
| ST0 Ti (Blank) | $^{48}$Ti | 60 | $^{48}$Ti ionic calibration<br>Linearity<br>**R² ≥ 0,999** |
| ST1 Ti (5 ppb) | $^{48}$Ti | 60 | |
| ST2 Ti (10 ppb) | $^{48}$Ti | 60 | |
| ST3 Ti (15 ppb) | $^{48}$Ti | 60 | |
| ST0 Ti (Blank) | $^{47}$Ti | 60 | $^{47}$Ti ionic calibration<br>Linearity<br>**R² ≥ 0,999** |
| ST1 Ti (5 ppb) | $^{47}$Ti | 60 | |
| ST2 Ti (10 ppb) | $^{47}$Ti | 60 | |
| ST3 Ti (15 ppb) | $^{47}$Ti | 60 | |
| Blank | $^{48}$Ti | 60 | **Same sample analyzed twice without delay (no rinsing sequence)** |
| Blank | $^{47}$Ti | 60 | |
| Sample 1 - C1.2µm D10000 | $^{48}$Ti | 60 | **Same sample analyzed twice without delay (no rinsing sequence)** |
| Sample 1 - C1.2µm D10000 | $^{47}$Ti | 60 | |
| 40 nm AuNP CONTROL #2 | $^{197}$Au | 60 | Size recovery : **95 – 105 %**<br>Number recovery : **80 – 120 %** |

## Additional data regarding sample preparation and spICP-MS analysis reliability and repeatability

Repeatability for both the sample preparation methodology and the spICP-MS analysis was demonstrated by repeating the entire protocol with different E171 food additives and final products. Reliability of the size measurement by spICP-MS was demonstrated through comparisons with scanning electron microscope (SEM) data. Table S4 presents the figures of repeatability for one E171 additive premix used as in-house control sample and Tables S4 and S5 present the figures of repeatability and reliability for two final products obtained through official sampling on the French market.

Relative standard deviations (RSDs) ≤ 5% were obtained for the mean and the median size measurements for the E171 additive premix (Table S4), the chewing gum coating (Table S5) and the chocolate candy coating (Table S6). These low RSDs demonstrated both intra-day and inter-day repeatability of the whole procedure for the E171 additive premix and final products with E171 containing coating.

Sizing accuracies (spICP-MS vs. SEM primary particle measurement) ranged between 93% and 98% for both the mean and the median size measurements of the chewing gum coating (Table S5) and the chocolate candy coating (Table S6). These good recoveries supported the reliability of the spICP-MS size measurements as well as the suitability of the sample preparation methodology for final products with E171 containing coating. In addition, the similarity between spICP-MS and SEM results supports the idea that only few aggregates are present in the prepared solutions.

**Table S4: Figures of repeatability obtained for in-house E171 additive premix used as spICP-MS control sample**

| | | | Mean size | | | $D_{50}$ – Median size | | |
|---|---|---|---|---|---|---|---|---|
| **In-house E171 additive premix used as spICP-MS control sample** | **Day #** | **Number of measurements** | **Mean (nm)** | **SD (nm)** | **RSD (%)** | **Mean (nm)** | **SD (nm)** | **RSD (%)** |
| | 1 | 1 | 173 | N/A | N/A | 162 | N/A | N/A |
| | 2 | 3 | 180 | 2,9 | 2% | 168 | 2,0 | 1% |
| | 3 | 2 | 174 | 2,8 | 2% | 164 | 3,5 | 2% |
| | 4 | 2 | 170 | 0,0 | 0% | 157 | 0,7 | 0% |
| | 5 | 3 | 167 | 3,1 | 2% | 156 | 3,1 | 2% |
| | 6 | 2 | 171 | 1,4 | 1% | 161 | 3,5 | 2% |
| | 7 | 5 | 174 | 3,0 | 2% | 161 | 1,9 | 1% |
| | 8 | 3 | 169 | 2,2 | 1% | 156 | 5,9 | 4% |
| | 9 | 3 | 170 | 6,0 | 4% | 156 | 7,1 | 5% |
| | 10 | 2 | 169 | 0,7 | 0% | 157 | 0,7 | 0% |
| | 11 | 2 | 166 | 1,4 | 1% | 154 | 0,7 | 0% |
| | **Global** | **28** | **172** | **4,8** | **3%** | **159** | **5,1** | **3%** |

**Table S5: Figures of repeatability and reliability (vs. SEM measurement) obtained by spICP-MS for a typical chewing gum tablet with white coating (analysis of the coating containing the E171 additive)**

| **Chewing gum spICP-MS** | **Replicate preparation** | **Dilution level** | **Mean diameter (nm)** | **D50 - Median size (nm)** |
|---|---|---|---|---|
| | 1 (Day 1) | 1 | 144 | 139 |
| | | 2 | 137 | 132 |
| | 2 (Day 1) | 1 | 143 | 139 |
| | | 2 | 137 | 131 |
| | 3 (Day 1) | 1 | 142 | 136 |
| | | 2 | 140 | 132 |
| | | **Mean (nm)** | **140** | **135** |
| | | **SD (nm)** | **2,8** | **3,6** |
| | | **RSD (%)** | **2,0%** | **2,7%** |
| **SEM analysis for confirmation 300 primary particles measured** | | | **137** | **127** |
| **% Sizing accuracy (spICP-MS vs. SEM)** | | | **98%** | **94%** |

**Table S6: Figures of repeatability and reliability vs. SEM measurement obtained by spICP-MS for a typical chocolate candy with peanut core and colored coating (analysis of the coating containing the E171 additive)**

| Chocolate candy spICP-MS | Replicate preparation | Dilution level | Mean diameter (nm) | D50 - Median size (nm) |
|---|---|---|---|---|
| | 1 (Day 1) | 1 | 125 | 110 |
| | | 2 | 129 | 113 |
| | 2 (Day 2) | 1 | 135 | 119 |
| | | 2 | 132 | 116 |
| | 3[a] (Day 3) | 1 | 133 | 120 |
| | | **Mean (nm)** | **131** | **116** |
| | | **SD (nm)** | **3,7** | **4,4** |
| | | **RSD (%)** | **2,8%** | **3,8%** |
| **SEM analysis for confirmation 300 primary particles measured** | | | **122** | **114** |
| **% Sizing accuracy (spICP-MS vs. SEM)** | | | **93%** | **98%** |

[a] Only one dilution level was analyzed on day 3

## Determination of $SiO_2$ content and particle concentrations in silica suspensions by ICP-OES

Silica microsphere suspensions (300, 500 and 1000 nm nominal diameters) were thoroughly homogenized and diluted 10-fold in ultrapure water. Then, 500 µL aliquots were digested in duplicate with 100 µL HF (40%w/w) and 5000 µL $HNO_3$ (69%w/w). 50 µL of internal standard (1000 µg mL$^{-1}$ Sc) were added to the resulting digests and the volume was brought to 50 mL with ultrapure water for ICP-OES analysis (Varian 720-ES equipped with Agilent OneNeb HF compliant nebulizer; Sc 361.383 nm and Si 288.158 nm). Calibration was achieved using Si standards (0.5 – 1 – 5 – 10 – 20 µg mL$^{-1}$) supplemented with Sc internal standard. For further calculations, Si/$SiO_2$ mass fraction was considered to be 46.7% and $SiO_2$ density 2.0 g cm$^{-3}$ (data provided by the manufacturer). Procedural blanks (*i.e.* 100 µL HF (40%w/w) + 5000 µL $HNO_3$ (69%w/w) + ultrapure water up to 50 mL) were analyzed and subtracted to the samples. Results are presented in Table S7.

$SiO_2$ particle concentrations are presented in Table S7 and were calculated according to the following equation:

$$SiO_2\ particle\ conc. = \frac{6 \times Cs}{10^{-18} \times Dp^3 \times \pi \times \rho}$$

where *$SiO_2$ particle conc.* is the target particle concentration (mL$^{-1}$), *Cs* is the $SiO_2$ concentration determined by ICP-OES (Table S7; mg mL$^{-1}$), *Dp* is the $SiO_2$ particle diameter provided by the manufacturer (nm) and $\rho$ is the density of the $SiO_2$ particles provided by the manufacturer (2.0 g cm$^{-3}$).

**Table S7: $SiO_2$ and particle concentrations in silica suspensions** – Uncertainties were calculated as the standard deviation of the duplicate values (n = 2 preparations).

| **$SiO_2$ particle diameter from manufacturer (nm)** | **$SiO_2$ conc. ICP-OES (mg $mL^{-1}$)** | **$SiO_2$ particle conc. ($mL^{-1}$)** |
|---|---|---|
| **299** | 90 ± 9 | $(3.2 \pm 0.3)10^{12}$ |
| **507** | 95 ± 8 | $(7.0 \pm 0.5)10^{11}$ |
| **1046** | 92 ± 9 | $(7.7 \pm 0.8)10^{10}$ |

**Sample B1 analysis with 10 millisecond dwell time** was performed in order to determine whether the detector saturation phenomenon also occurred with this higher integration duration. Fig. S1 shows the $TiO_2$ PSDs obtained for sample B1 when acquiring $^{47}Ti$ and $^{48}Ti$ signals at 10 ms dwell time. Both $^{47}TiO_2$ and $^{48}TiO_2$ PSDs were very similar and all the following observations are comparable to those obtained with 100 µs dwell time. Indeed, very few particles (*i.e.* 23 out of 1195 particles) were detected below 100 nm and the frequency hardly reached a maximum of 7 for $^{48}Ti$ at 70 nm and 90 nm. From 100 nm up to 200 nm, both $^{48}TiO_2$ and $^{47}TiO_2$ frequencies overlapped quite well and increased steadily. Above 200 nm, $^{47}TiO_2$ and $^{48}TiO_2$ PSDs diverged significantly. $^{48}TiO_2$ PSD increased steeply to reach a maximum frequency of 117 at 280 nm and collapsed rapidly ending around 400 nm while $^{47}TiO_2$ PSD was shaped like a Gaussian curve (solid black line in Fig. S1) spreading from 100 nm up to 600 nm and centered on 352 nm with an average maximum frequency of 48 and a standard deviation of 94 nm (obtained with OriginPro 2015 software). The local maximum of the $^{47}TiO_2$ PSD frequency is 55 at 350 nm. Combination of $^{48}TiO_2$ (≤ 150 nm) and $^{47}TiO_2$ (> 150 nm) PSD is presented as a solid blue line on Fig. S1 and once again is very similar to the one obtained with 100 µs dwell time. These observations demonstrated that the saturation of $^{48}Ti$ signal for larger $TiO_2$ particles was not limited to microsecond dwell time but might also appear using millisecond dwell times.

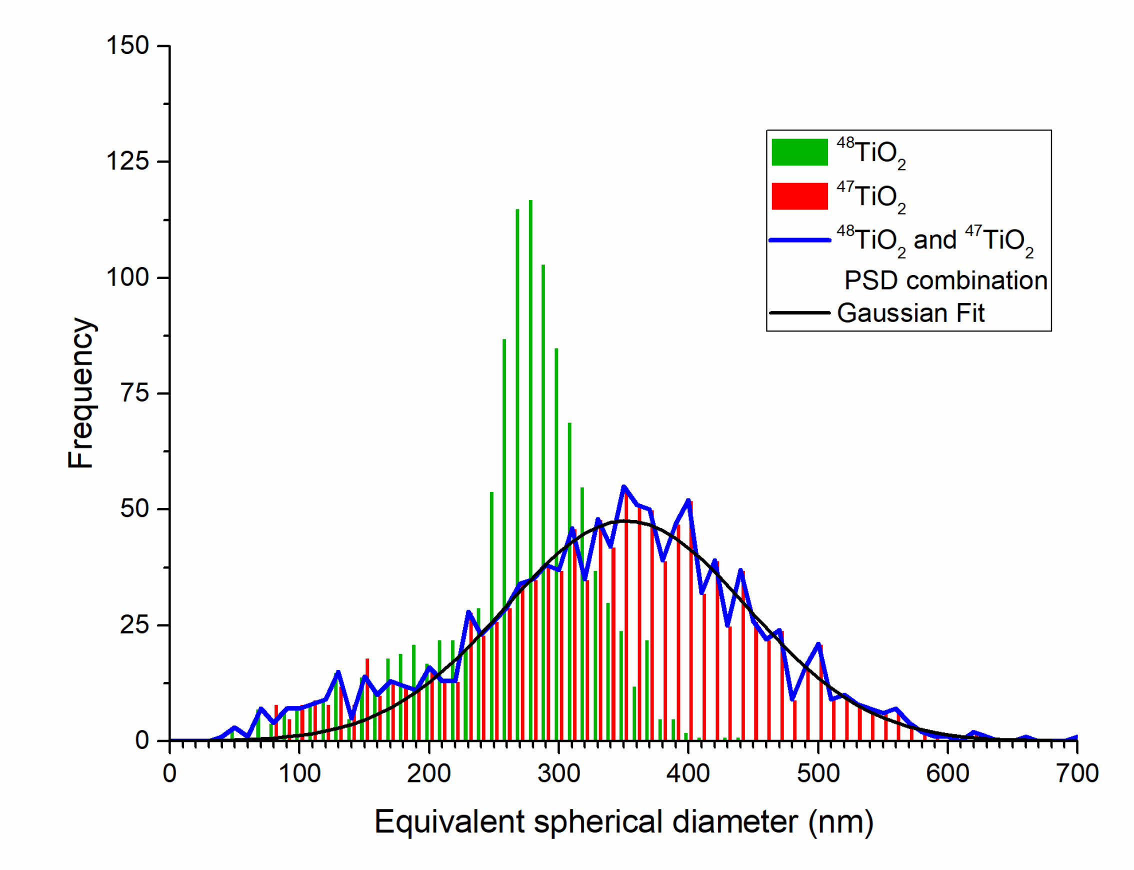

**Fig. S1: $TiO_2$ PSD of sample B1 with 10 ms dwell time** - $^{47}TiO_2$ and $^{48}TiO_2$ PSDs of sample B1, PSD combination (*i.e.* $^{48}TiO_2$ data ≤ 150 nm and $^{47}TiO_2$ data > 150 nm) as solid blue line and Gaussian fitting (OriginPro 2015 software) of the PSD combination as solid black line.

**Table S8: Physico-chemical properties of Ti, $TiO_2$, Si and $SiO_2$** (ranges are provided when different values are reported in the literature especially depending on the crystallographic form *e.g.* $TiO_2$ rutile vs. anatase, $SiO_2$ amorphous vs. quartz)

| Material | Molecular weight (g $mol^{-1}$) | Usual density range (g $cm^{-3}$) | Melting point (°C) | Boiling point (°C) | Ionization Energy (eV) |
|---|---|---|---|---|---|
| **Ti** | 47.87 | 4.51 | 1668 | 3287 | 6.8281 (Ti) |
| **$TiO_2$** | 79.87 | 3.79 - 4.23 | 1843<br>(1560 - 1912) | 2972 | 7.8 - 9.5 ($TiO_2$) |
| **Si** | 28.09 | 2.33 | 1414 | 3265 | 8.1517 (Si) |
| **$SiO_2$** | 60.08 | 1.9 - 2.7 | 1713 - 1722 | 2950 | 11.8 - 12.6 ($SiO_2$) |

All data (except some ionization energy data for $TiO_2$ and $SiO_2$) are from Handbook of Chemistry and Physics 89th edition (edited by David R. Lide) and NIST online Chemistry WebBook n°69 (https://doi.org/10.18434/T4D303 - last access 19/12/2018).
Additional ionization energy data from Scanlon *et al.* (2013), Maj *et al.* (1988) and Kostko *et al.* (2009).

**Fig. S2: Illustration of spICP-MS signal saturation** - Raw data (10 s section extract) for sample B1, comparison of raw signal (spikes) during $^{48}$Ti (a) and $^{47}$Ti (b) acquisition. Example of a $TiO_2$ particle clipped spike with detector saturation around 1400 counts during $^{48}$Ti acquisition (c).

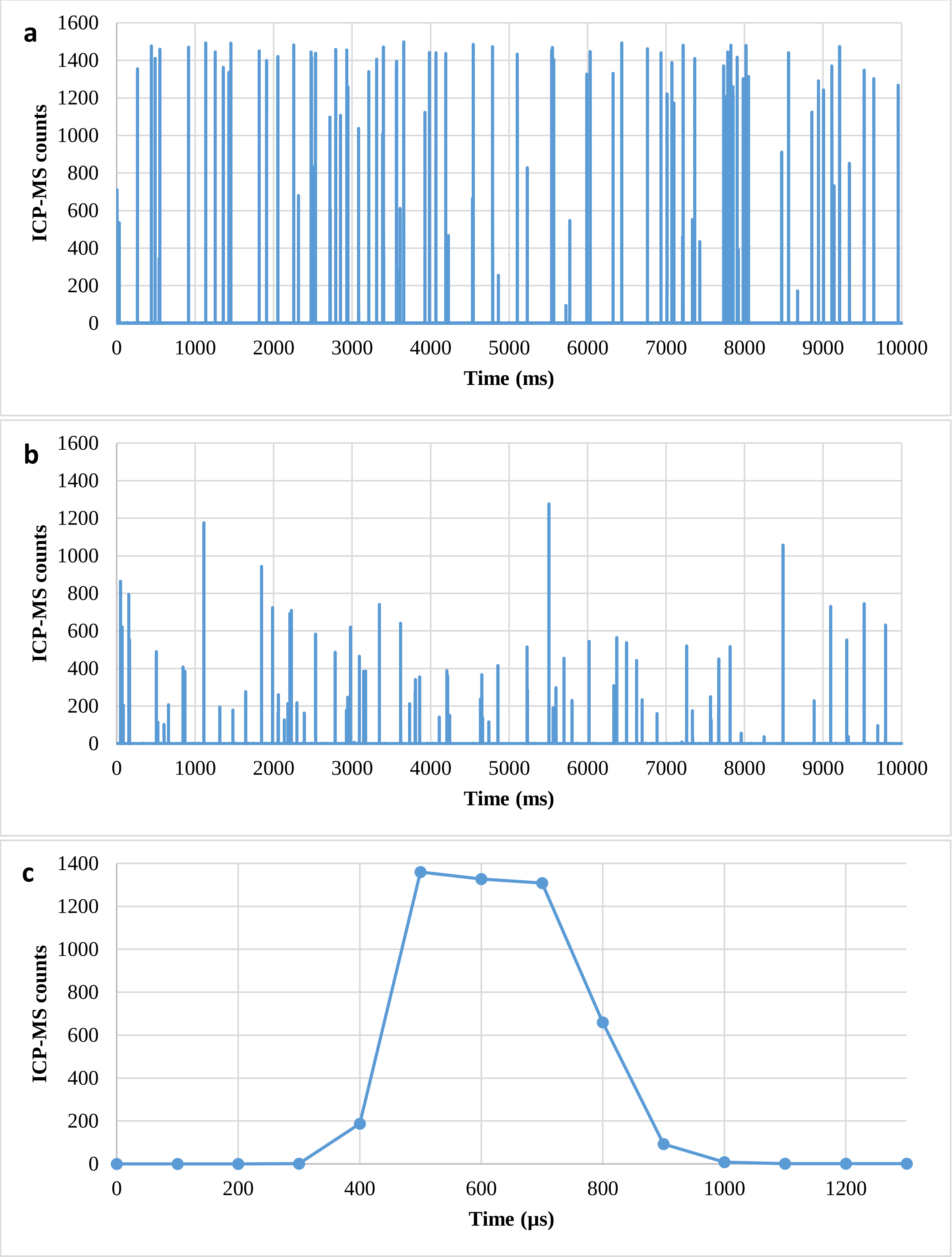

1. e. David R. Lide, *CRC Handbook of Chemistry and Physics, 89th Edition (Internet Version 2009)*, CRC Press/Taylor and Francis, Boca Raton, FL, 2009.
2. L. J. Gimbert, P. M. Haygarth, R. Beckett and P. J. Worsfold, *Environmental Science & Technology*, 2005, **39**, 1731-1735.
3. D. O. Scanlon, C. W. Dunnill, J. Buckeridge, S. A. Shevlin, A. J. Logsdail, S. M. Woodley, C. R. A. Catlow, M. J. Powell, R. G. Palgrave, I. P. Parkin, G. W. Watson, T. W. Keal, P. Sherwood, A. Walsh and A. A. Sokol, *Nature Materials*, 2013, **12**, 798.
4. S. Maj, *Physics and Chemistry of Minerals*, 1988, **15**, 271-273.
5. O. Kostko, M. Ahmed and R. B. Metz, *The Journal of Physical Chemistry A*, 2009, **113**, 1225-1230.